Swirling Flow in a Research Combustor

J. I. Ramos* and H. T. Somer†
Carnegie-Mellon University, Pittsburgh, Pennsylvania

Measurements of turbulent, confined, swirling flows have been obtained by means of a two-color laser Doppler velocimeter in a research combustor and compared with other experimental data and numerical results obtained by means of two two-equation models of turbulence. The combustor consists of two confined, concentric, swirling jets whose mass flow rates and swirl numbers can be controlled independently, and which can be used to study cold flow, premixed and non-premixed reactive flows, and two-phase flows. Results are reported for cold flow conditions under co- and counterswirl. It is shown that under both conditions a closed recirculation zone is created at the combustor centerline. This zone is characterized by the presence of a one-celled toroidal vortex, low tangential velocities, high turbulent intensities, and large dissipation rates of turbulence kinetic energy. The experimental data agree satisfactorily with the numerical results, but do not agree with other experimental data under coswirl flow conditions. The reasons for the discrepancies are discussed.

Introduction

An important application of swirling flows lies in its use to provide flame stabilization and improved mixing in many combustion chambers.[1] In order to achieve enhanced flame stabilization and better control of the mixing process, multiple coaxial swirling streams can be introduced in swirl combustors. Yetter and Gouldin[2] carried out a series of experiments on a model combustor which uses two coaxial swirling jets. They found that the fluid mechanical aspects play an important role in determining the operation of the combustor; combustion under coswirl conditions (jets rotating in the same direction) was found to be significantly different from combustion under counterswirl conditions. Vu and Gouldin[3] performed experiments in a model combustor composed of two confined coaxial swirling jets under nonreacting conditions. They found that a recirculation zone occurs only with counterswirl near the exit of the inner jet. The recirculation zone was in the form of a one-celled toroidal vortex having very low swirl velocities. Habib and Whitelaw[4] performed similar experiments in confined coaxial jets although under weak swirl conditions, i.e., no recirculation zone at the combustor centerline appeared in their experimental work. Gouldin et al.[5] performed experiments similar to those reported here and in Ref. 3 by means of a laser Doppler velocimeter (LDV) and found that a recirculation zone is created at the combustor centerline only under counterswirl flow conditions. The results of Gouldin et al.[5] and Vu and Gouldin[3] indicate that, in the geometrical arrangement employed by these investigators, coswirl does not result in a recirculation zone under incompressible flow conditions. The results presented in this paper show that a recirculation does exist under both co- and counterswirl flow conditions.

Experimental work on turbulent, confined, swirling flows has also been performed by Rhode,[6] Rhode et al.,[7] Gupta et al.,[8] and Yoon and Lilley.[9] Rhode[6] and Rhode et al.[7] studied swirling flows in a combustor provided with a sudden expansion by means of a visualization technique in which neutrally buoyant helium filled soap bubbles were employed. The results of the visualization technique were compared with a two-equation model of turbulence and showed that the model predicts the gross features of the flowfield. Gupta et al.[8] modeled a magnetohydrodynamic (MHD) swirl combustor and obtained good agreement between the theoretical predictions obtained by means of a two-equation turbulent model and the qualitative experimental results which were obtained by means of a visualization technique. Yoon and Lilley[9] employed a five-hole pitot probe to measure the mean velocity profiles in confined swirling flows and showed that, in a combustor provided with a sudden expansion, a recirculation zone is created at the combustor centerline. This recirculation zone is, in some cases, followed by a precessing vortex core. Yoon and Lilley[9] also investigated the effects of a downstream contraction on the centrally-located recirculation zone and showed that the recirculation zone is shortened by the downstream contraction.

In a recent experimental study, Sommer[10] employed LDV to measure the mean velocity field and Reynolds stresses in a research combustor similar to that employed by Vu and Gouldin[3] and Gouldin et al.,[5] and showed that a recirculation is created at the combustor centerline under both co- and counterswirl flow conditions. This recirculation zone has the form of a one-celled toroidal vortex. Sommer's[10] experimental results for coswirl flow conditions are distinctly different from those of Vu and Gouldin[3] and Gouldin et al.,[5] who employed hot-wire anemometry and LDV, respectively. They should also be compared with the experimental data obtained by Yetter and Gouldin[2] who showed that a recirculation zone does exist for both co- and counterswirl under reacting flow conditions. The results of Vu and Gouldin,[3] Gouldin et al.,[5] and Yetter and Gouldin[2] indicate that the flowfield in a swirling flow combustor is very sensitive to the chemical heat release in that under incompressible flow conditions a recirculation zone is observed only under counterswirl, while under reacting (premixed) flow conditions a recirculation zone is observed under both co- and counterswirl.

In addition to the experimental work on confined swirling flows reported in the previous paragraphs, there has been a great interest in predicting such flows because of their importance in increasing the rates of mixing and reaction in practical combustors.[1] For example, Habib and Whitelaw[4] employed a k/ϵ model of turbulence and compared their numerical predictions with experimental data under weak swirl flow conditions. Habib and Whitelaw[4] found that the turbulence model employed in their calculations was unable to predict the experimentally observed velocity minimum at the centerline of their combustor model. This inability was attributed to the lack of streamline curvature effects in their turbulence model and to the inappropriateness of an isotropic turbulent viscosity in swirling flows.

Presented as Paper 83-0313 at the AIAA 21st Aerospace Sciences Meeting, Reno, Nev., Jan. 10-13, 1983; received July 1, 1983; revision received Dec. 11, 1983.

*Assistant Professor of Mechanical Engineering. Member AIAA.
†Professor of Mechanical Engineering. Member AIAA.

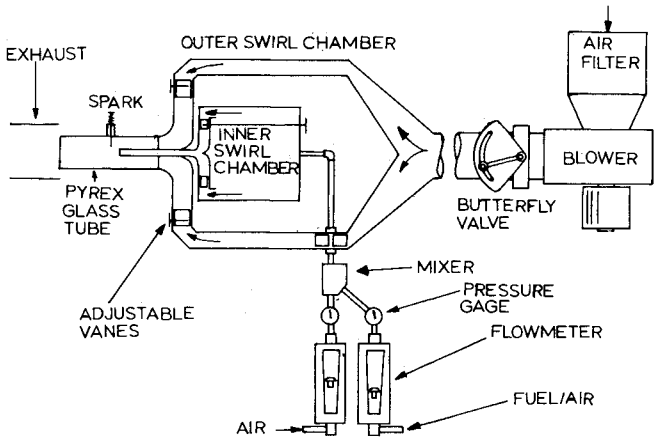

Fig. 1 Schematic of the swirl combustor.

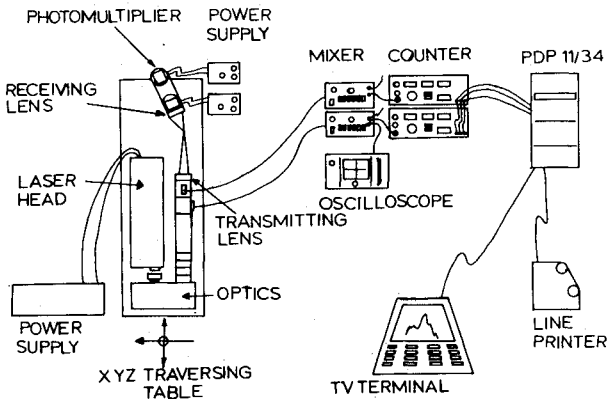

Fig. 2 Schematic of the LDV and data acquisition systems.

Kubo and Gouldin[11] developed a numerical technique for solving axisymmetric, incompressible, turbulent swirling flows. They used the steady state conservation equations in terms of the vorticity and streamfunction, and showed that a recirculation zone appears under co- and counterswirl flow conditions.

Similar results were found by Ramos[12-17] using the k/ϵ and k/ℓ models of turbulence, where k and ϵ are the turbulence kinetic energy and the dissipation rate of turbulence kinetic energy, and ℓ is the turbulent length scale. From the numerical results of Kubo and Gouldin,[11] and Ramos,[12-17] it was concluded that the k/ϵ and k/ℓ models of turbulence (with the set of constants used in these works) predicted a recirculation zone at the combustor centerline under coswirl conditions, whereas the experimental data of Vu and Gouldin[3] do not show such a recirculation zone.

Similar results were found by Srinivasan and Mongia,[18] who employed the inlet boundary conditions experimentally measured by Vu and Gouldin[3] and found that, with these boundary conditions, the k/ϵ model employed in their calculations was unable to predict a recirculaton zone under both co- and counterswirl flow conditions. In order to predict a recirculation zone at the combustor centerline, Srinivasan and Mongia[18] found it necessary to include the effects of streamline curvature in their turbulence model by means of a curvature Richardson number. The introduction of such a number resulted in a recirculation zone for both co- and counterswirl flow conditions. The numerical results were found to be in agreement with the experimental data of Ref. 3 only for counterswirl. For coswirl flow conditions their modified k/ϵ model predicted a recirculation zone that had not been observed by Vu and Gouldin.[3] Ramos[14-17] employed the k/ϵ and k/ℓ models of turbulence and compared the numerical predictions with the experimental data of Vu and Gouldin.[3] He showed that both models can predict a recirculation zone at the combustor centerline under both co- and counterswirl flow conditions if appropriate inlet boundary conditions are employed in the calculations, even when the effects of the streamline curvature are not included in the turbulence models. For example, Ramos[14-17] showed that both the k/ϵ and k/ℓ models are unable to predict a recirculation zone for both co- and counterswirl flow conditions if a solid body rotation is employed for the inner jet tangential velocity profile at the combustor inlet. However, if the azimuthal velocity profile of the inner jet is assumed to consist of a combination of a solid body rotation and a free vortex structure, then both models predict a recirculation zone at the combustor centerline under both co- and counterswirl flow conditions.[12-17] Ramos[14,17] compared the numerical predictions of the k/ϵ and k/ℓ models with the experimental data of Ref. 3 and obtained good agreement for counterswirl flow conditions. For coswirl, the numerical calculations predicted a recirculation zone which was not observed in Ref. 3. Sommer[10] compared his LDV data with the numerical results of Ramos[14] and showed that the experimental data are in good agreement with the numerical predictions. Sommer's[10] experimental data were also found in good agreement with those of Vu and Gouldin[3] for counterswirl flow conditions, but showed a recirculation zone under coswirl which had not been found by Vu and Gouldin.[3]

In this paper the axisymmetric, turbulent, swirling flowfield in a research combustor is studied both experimentally[10] and numerically.[14] The combustor consists of two concentric pipes and can operate under co- and counterswirl flow conditions. Measurements of the mean axial velocity, mean tangential velocity, turbulence intensity, and Reynolds stresses have been obtained by means of a two-color laser Doppler velocimeter that measures the axial and tangential velocity components simultaneously. Measurements are presented for nonreacting (cold) flows under both co- and counterswirl conditions.[10] These measurements are compared with the numerical results obtained by means of two two-equation turbulence models.[14-17] These models use an isotropic eddy diffusivity and solve equations for the turbulence kinetic energy and for the turbulent length scale.[17] Both the experimental and numerical results are compared with those obtained by Vu and Gouldin[3] in a similar geometrical arrangement by means of a hot-wire anemometer.

The experimental data presented here are believed to be very important for the validation of numerical predictions of confined swirling flows. This validation is necesary if the numerical models are to predict the flowfield in more complex geometrical arrangements under reactive flow conditions. In addition, a validation of the numerical predictions of incompressible (cold) swirling flows is necessary before investigating the flowfield in reactive swirling flows. Such a validation is presented here. However, due to space limitations, the turbulent models, governing equations, and boundary conditions are not shown in this paper; they can be found in Refs. 12-14.

Experimental Apparatus

The experimental setup consists of a research combustor, a two-color laser Doppler velocimeter system, and signal procesing hardware and software. A brief description of these three components of the experimental apparatus is given in the following sections.

Combustor Facility

The experimental apparatus was built to study complex swirling flow systems whose mass flow rate, swirl number,

and initial turbulence level can be controlled. The experimental setup used to generate a controllable swirl-stabilized flow consists of three sections: a combustion air supply section, a swirl generating section, and the test section (Fig. 1).

A high pressure head centrifugal air blower provides a maximum flow rate of 2576 m^3/h (91,000 ft^3/h) to cover the Reynolds number range of interest (10^4-10^5). The air is filtered through a high efficiency filter system to clean it of uncontrolled particles. The flow rate is controlled by a calibrated butterfly valve. A 4.60 m (15 ft) long, 20 cm (8 in.) diam pipe connects the blower with the swirl generating section. Flow straighteners (honeycomb) are installed to provide a fully developed turbulent flow with a uniform velocity profile at the entrance of the swirl generator section.

The outer swirl chamber consists of an annular passage of constant cross-sectional area to reduce pressure drops and a 24 adjustable vane swirl generator. The vanes introduce a tangential velocity component to create the swirl in the test section. The inner swirl chamber is designed in the same way so that a supply of swirling fuel gas and/or air and co- and counterswirl flows can be investigated in the test section. The third section of the experimental apparatus consists of a pyrex glass tube in which the two swirling flows interact. In this region, a spark plug can be used to ignite the combustible mixture in the recirculation zone. The pyrex glass tube discharges the air or reaction products into an exhaust system. As indicated in Fig. 1, the inner swirl flow can contain premixed fuel and air so that reacting flow experiments can be performed in the same experimental apparatus.

Laser-Doppler Velocity Diagnostics

A schematic of the laser Doppler velocimeter system is shown in Fig. 2. A LEXEL two-color argon-ion laser provides the monochromatic and coherent light sources. It gives up to 4 W of fundamental mode power for both the green (514.5 nm) and the blue (488.0 nm) color beams. The beams are then collimated to keep a divergence angle within 0.3 mrad. Color separation, polarization, and beam splitting are all done in TSI modules, which are optically shielded to block out the background noise.

Acousto-optical frequency-shifting devices are implemented to circumvent highly fluctuating velocities and/or directional ambiguity. Two separate sets of frequency shifters with Bragg cells are used to prevent cross-talk between the two channels. The four beams are then focused to a small probe volume by the transmitting lens, which has a focal length of 242 mm. This probe volume is ellipsoidal in shape with major and minor axes of 1.69 mm and 0.164 mm, respectively. Because of the strong reflection due to the round glass tube and high velocity fluctuations, it was decided to use forward scattering instead of backward scattering, which usually lowers the signal-to-noise ratio.

In neglecting the effect of particle dynamics, it was also assumed that the particle velocities represent the local fluid velocities. The shape, size, and scattering properties of the particles and the environment greatly affect the signals received by the photomultiplier. In the cold flow experiments reported here, aluminum oxide particles of diameters of about 0.3 μm were used to seed the flow, and proved to be satisfactory at a laser power of 1 W.

The light scattered by these particles is collected through the receiving lens with a focal length of 242 mm and then filtered and separated into the two colors again. To avoid direct illumination from the transmitting beams, the axis of the receiving optics forms an angle of 15 deg with that of the transmitting optics. The fringe spacing is 5.67 μm for the blue color and 5.94 μm for the green color.

Two photomultipliers with high quantum efficiency (22%) and high sensitivity (300 μA/lm) convert the photon signal to electric signal which is then downmixed in the frequency shifter and processed by the counter. The downmixer allows a 0 - 10 MHz range of effective frequency shifting. Since the green channel is chosen to measure the velocity in the tangential direction and the blue channel that in the axial direction, frequency shifting is 5.0 MHz for the green channel and 2.0 MHz for the blue one.

Signal Processing

TSI counters are used to process the Doppler signals and are connected to a PDP 11/34 mincomputer. The counters

1 DATE OF EXPERIMENT	02-NOV- 81
2 TIME OF EXPERIMENT	03:57:57
3 DATA COLLECTED IN FILE	001 .SUV
4 X-COORDINATE IN CMS	1.000
5 Y-COORDINATE IN CMS	0.000
6 Z-COORDINATE IN CMS	0.000
7 NUMBER OF RECORDS COLLECTED IN THIS RUN	1191.
8 MODE TYPE	COINCIDENCE
9 FREQUENCY SHIFTED IN MHZ (CH1)	2.000
10 FREQUENCY SHIFTED IN MHZ (CH0)	5.000
11 FREQUENCY SPACING IN MHZ (CH1)	5.670
12 FREQUENCY SPACING IN MHZ (CH0)	5.940

RESULTS OF CALCULATIONS:

	MINIMS	MAXIMS	MEANZ	RMSS	SKEWN-S	FLATN-S
U-COMPONENT:	2.906	43.442	29.874	4.841	- .507	4.386
W-COMPONENT:	-22.836	33.407	9.343	14.047	- .658	2.218
V(ABS.VEL.):	11.712	47.860	34.282	5.031	- .469	3.878
UW:	-531.164	364.508	-8.592	66.849	- .189	9.243
SIN(U,V):	.099	1.000	.874	.095	-1.015	6.636

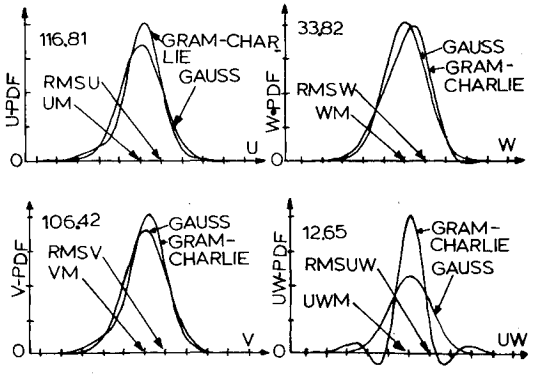

Fig. 3 Typical computer output for one point in the flow.

1 DATE OF EXPERIMENT	02-NOV-81
2 TIME OF EXPERIMENT	03:57:57
3 DATA COLLECTED IN FILE	001 .SUV
4 X-COORDINATE IN CMS	1.000
5 Y-COORDINATE IN CMS	0.000
6 Z-COORDINATE IN CMS	0.000
7 NUMBER OF RECORDS COLLECTED IN THIS RUN	1191.
8 MODE TYPE	COINCIDENCE
9 FREQUENCY SHIFTED IN MHZ (CH1)	2.000
10 FREQUENCY SHIFTED IN MHZ (CH0)	5.000
11 FREQUENCY SPACING IN MHZ (CH1)	5.670
12 FREQUENCY SPACING IN MHZ (CH0)	5.940

RESULTS OF CALCULATIONS:

	MINIMS	MAXIMS	MEANZ	RMSS
U-COMPONENT:	2.906	44.442	29.874	4.841
W-COMPONENT:	-22.836	33.407	9.343	15.047
V(ABS.VEL.):	11.712	47.860	34.282	5.031
UW:	-531.164	364.508	-8.592	66.849
SIN(U,V):	.099	1.000	.874	.095

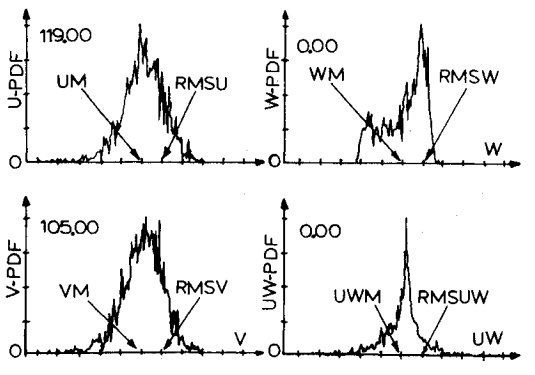

Fig. 4 Typical probability density function of the experimental data.

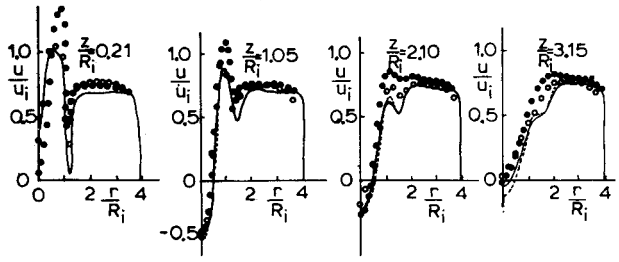

Fig. 5 Mean axial velocity profiles for counterswirl: ●, Vu and Gouldin[3] hot-wire data; –, k/ℓ model - -, k/ϵ model; ○, LDV data.

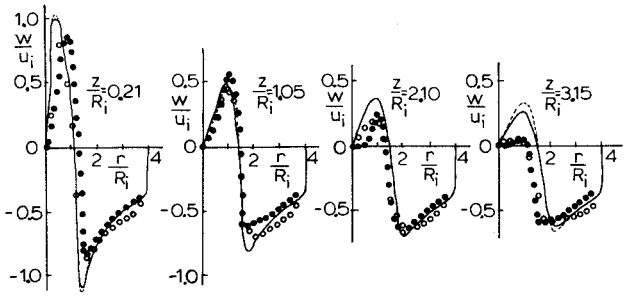

Fig. 6 Mean tangential velocity profiles for counterswirl: ●, Vu and Gouldin[3] hot-wire data; –, k/ℓ model; - -, k/ϵ model; ○, LDV data.

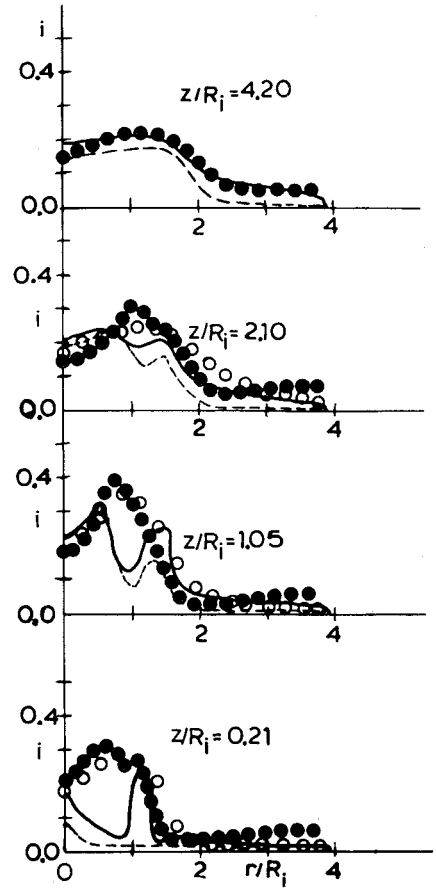

Fig. 7 Turbulent intensity profiles for counterswirl; ●, Vu and Gouldin[3] hot-wire data; –, k/ℓ model; - -, k/ϵ model; ○, LDV data.

eliminate invalid data by setting thresholds and by comparing levels on both amplitude and time coordinates. An interfacing buffer between counters and computer measures the time between data information and sets a time window to make sure that the two counters are viewing the same particle. Data rate of validated counts is kept in the range of about 1000/s.

Two groups of interactive programs written in FORTRAN have been developed. The on-line data collecting procedure allows an instantaneous brief check of mean velocity and velocity rms with a histogram plot. This program directs the computer to accept up to 4000 valid velocity values and to store them in its memory. A statistical representative set of these values is used to obtain the velocity and turbulence information.

A program was developed to perform a complete statistical analysis of the laser Doppler velocimeter data of both velocity components. It predicts the first four statistical moments of the data, and reconstructs the probability density function assuming Gaussian and Gram-Charlie distributions. Figure 3 shows a typical computer output for one point in the flow. A total of 1181 individual velocity values for each component were analyzed. An average velocity of 29.87 m/s in the axial direction (u) was observed with a velocity rms of 4.84 m/s. The tangential velocity component (w) was measured to be 8.34 m/s with a velocity rms of 14.05 m/s. Mean and velocity rms values and Reynolds stresses were calculated and their distributions plotted.

Figure 4 corresponds to Fig. 3 and shows the probability density distribution of the real data. Figures 3 and 4 represent a typical record of a velocity-turbulence measurement at one point in the test section. Similar records were obtained at the other locations reported in this paper.

Presentation of Results

Some of the measured results are shown in Figs. 5-12 and are compared with the experimental data of Vu and Gouldin.[3] They are also compared with the numerical results obtained by means of the k/ϵ and k/ℓ models, where k is the turbulent kinetic energy, ϵ is the dissipation rate of turbulent kinetic energy, and ℓ is the turbulent length scale. The governing equations and boundary conditions employed in the numerical calculations are reported in Refs. 12-14. Reference 14 contains a summary of the models and boundary conditions employed in the calculations reported here. Due to space limitations, the governing equations and boundary conditions used in the calculations are not reported here; they can be found in Refs. 12-14.

Figures 5-8 correspond to counterswirl flow conditions in which the mean axial velocity profiles at the combustor inlet are uniform and equal to 30 and 20 m/s for the inner and outer jets, respectively. (The swirl number is defined as the ratio of the axial flux of the azimuthal momentum to that of the axial momentum.) Figures 9-12 show the mean axial and tangential velocity profiles, turbulent intensity profiles, and Reynolds stresses at different axial locations along the combustor for co-swirl flow conditions. These measurements correspond to swirl numbers of 0.58 and 0.54 for the inner and outer jets, respectively. The mean axial velocities of the inner and outer jets at the combustor inlet are 30 and 20 m/s, respectively. All of the measurements reported in Figs. 5-12 were obtained in a research combustor which consisted of a 3.72 cm diam inner pipe and a 14.50 cm diam outer pipe. The combustor length was 116 cm.

In Figs. 5-12, the mean axial velocity (u) profiles have been normalized by the inner jet axial velocity at the combustor inlet (u_i). These profiles are shown as a function of the radial distance (r) which has been normalized by the inner pipe radius (R_i). They are shown at several axial locations (z) along the combustor centerline. The axial locations have been normalized by the inner pipe radius. The tangential velocity (w) has also been normalized by the inner jet axial velocity at the combustor inlet, while the turbulent intensity profiles were calculated from $i=\sqrt{2k/3}/u_i$, where i is the turbulent intensity. The correlation $u'w'$, where u' and w' denote fluctuating axial and tangential velocity components, has also

been normalized by the product of the square root of $\overline{u'^2}$ and $\overline{w'^2}$, where an overbar stands for ensemble-averaged values. The LDV results presented in Figs. 5-12 indicate that the flowfield was axisymmetric, while the hot wire anemometry data of Vu and Gouldin[3] show that their flow is not exactly axisymmetric. The experimental data of Vu and Gouldin[3] presented in Figs. 5-12 are the averaged values of those obtained by these investigators on both sides of the combustor symmetry axis.

In Fig. 5 we show the mean axial velocity profiles at four axial locations as a function of the normalized radial distance. This figure indicates that at $z/R_i = 0.21$, the axial velocity profiles present two minima; one of them is located at the centerline, while the other occurs at $r/R_i = 1.0$ and is due to the finite thickness of the inner pipe. The velocity minimum at the combustor centerline is due to the centrifugal forces that lift the inner jet and, eventually, produce a recirculation zone as shown in Fig. 5 at $z/R_i = 1.05$, 2.10, and 3.15. Figure 5 also indicates that the mean axial velocity values obtained with the LDV system are smaller than those obtained by Vu and Gouldin[3] by means of a hot-wire anemometer. This is particularly noticeable in the inner jet at $z/R_i = 0.21$, where the normalized axial velocity profile obtained with hot-wire is about 30% larger than that obtained with LDV. Figure 5 also shows that the centerline velocity at $zR_i = 0.21$ is smaller in the experimental apparatus of Vu and Gouldin[3] than in the one presented here. The numerical results obtained with the k/ϵ and k/ℓ models are in very good agreement with each other and with the LDV data in the inner jet. However, they are in slightly better agreement with the hot-wire data in the outer jet. It should be pointed out that the inlet boundary conditions employed in the calculations presented here are not those of the experiments. The inlet boundary conditions were selected to give the best overall agreement with the experimental data of Vu and Gouldin[3] for counterswirl flow conditions without introducing curvature effects in the two-equation models of turbulence.

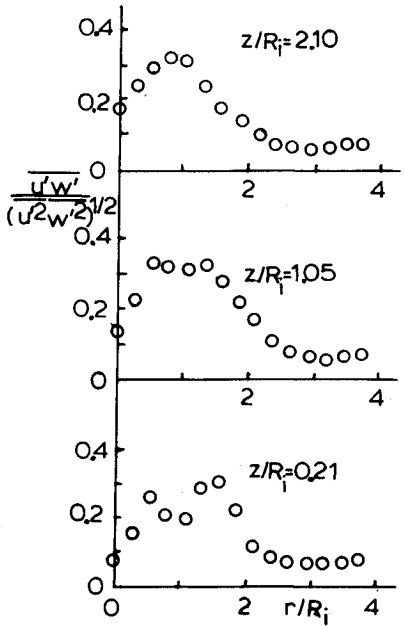

Fig. 8 Normalized axial-tangential velocity correlation profiles for counterswirl.

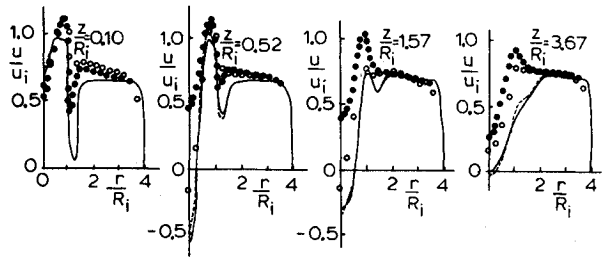

Fig. 9 Mean axial velocity profiles for coswirl: ●, Vu and Gouldin[3] hot-wire data: –, k/ℓ model; - -, k/ϵ model; ∘, LDV data.

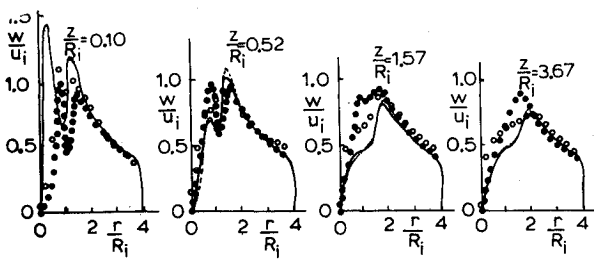

Fig. 10 Mean tangential velocity profiles for coswirl: ●, Vu and Gouldin[3] hot-wire data; –, k/ℓ model; - -, k/ϵ model; ∘, LDV data.

In Fig. 6 we present the nondimensional tangential velocity profiles at different axial locations along the combustor centerline for counter-swirl flow conditions. The LDV data are in reasonable agreement with Ref. 3 particularly in the inner jet. Both the tangential velocity values measured with the LDV and hot wire are approximately equal. However, at $z/R_i = 0.21$, the LDV data show that the tangential velocity of the inner jet presents a maximum closer to the combustor centerline than the hot wire data. This behavior is also observed in the numerical predictions which overpredict the velocity peaks. The agreement between the LDV and hot wire data improves downstream, i.e., at $z/R_i = 1.05$, 2.10, and 3.15. However, some discrepancies between the LDV and hot wire data are observed in the outer jet region whose free vortex tangential velocity profile decays much more slowly than that of the inner jet. The numerical results obtained with the k/ϵ and k/ℓ models differ little from each other but are in better agreement with the hot wire data than with the LDV data.

In Fig. 7 we show the turbulent intensity profiles at three axial locations. The turbulent intensity profiles obtained with the hot-wire anemometer are in good agreement with the LDV data in the inner jet region. These profiles show a peak at $r/R_i = 1.0$, i.e., at the interjet shear layer, which is mainly due to the turbulence production there. Figure 7 also shows that the recirculation zone is characterized by large levels of turbulence that decay downstream of the combustor inlet. The numerical calculations show substantial differences with the hot-wire and LDV data. These discrepancies are shown in Fig. 7 at $z/R_i = 0.21$ and 1.05 and are characterized by the presence of two turbulent intensity peaks. One of the peaks is located at the interjet shear layer, while the other is located in the recirculation zone and is associated with the radial gradients of the axial and tangential velocities at the combustor centerline as shown in Figs. 5 and 6.

We now turn our attention to the coswirl flow conditions shown in Figs. 9-12. In Fig. 9, we present the normalized mean axial velocity profiles as a function of the normalized radial coordinate at four axial locations along the combustor centerline. This figure indicates that there are substantial differences between the hot wire and LDV data and numerical predictions. Both the LDV data and the numerical predictions show a recirculation zone at the combustor centerline, e.g., at $z/R_i = 0.52$ and 1.57. However, the magnitude of centerline velocity predicted by the numerical calculations is larger than that measured by the LDV. The numerical results are in qualitative agreement with the LDV data. However, both are in disagreement with the hot-wire data of Vu and Gouldin[3] in that the LDV measurements and numerical calculations show that a recirculation zone does exist at the combustor centerline under coswirl flow conditions, whereas the hot-wire data do

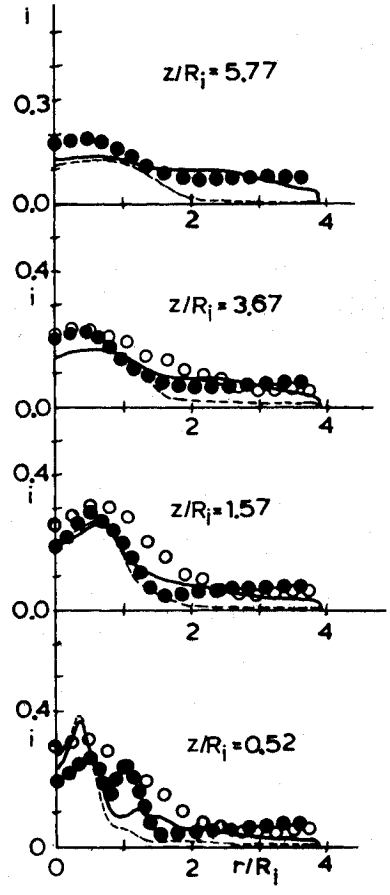

Fig. 11 Turbulent intensity profiles for coswirl: ●, Vu and Gouldin[3] hot-wire data; –, k/ℓ model; - -, k/ϵ model; ∘, LDV data.

not show such a recirculation zone. One could attribute the differences between the hot-wire and LDV data to the disturbances introduced by the hot wire probe and the fact that the flow direction is very complex, so that the hot-wire data are not very accurate. (The hot-wire anemometer is not sensitive to the flow velocity direction.) For example, Vu and Gouldin[3] estimate that at the centerline where the turbulent intensity is higher than 30%, errors of about ±20-50% are expected. However, in a recent paper, Gouldin et al.[5] studied the flowfield in the same combustor as Vu and Gouldin[3] by means of an LDV and showed that there is no recirculation zone at the centerline of their combustor under cold flow coswirl conditions. Since both Ref. 5 and the experiments reported here were performed in a similar arrangement, the reasons for the discrepancies in the velocity measurements may be attributed to the different methods employed to generate swirl in both experiments which also produce different inlet boundary conditions. Since the same swirl number was employed in both experiments, the hot-wire and LDV data indicate that the swirl number is not the only parameter that controls the flowfield in a swirl combustor, and that the flowfield is very sensitive to the inlet velocity profiles. Similar sensitivity has been observed in the numerical experiments of Rhode,[6], Ramos,[14-17] Srinivasan and Mongia,[18] Abujelala and Lilley,[19] and Sturgess et al.[20] For example, Ramos[14-17] showed that a tangential velocity profile consisting of a solid body rotation in the inner jet does not produce a recirculation at the combustor centerline for both co- and counterswirl flow conditions when turbulence models are applied to swirling flows without modification. Similar results were found by Srinivasan and Mongia,[218] who included a curvature Richardson number effect in the k/ϵ model and predicted a recirculation zone for both co- and counterswirl flow conditions when the experimentally measured inlet boundary conditions were employed in the numerical calculations.

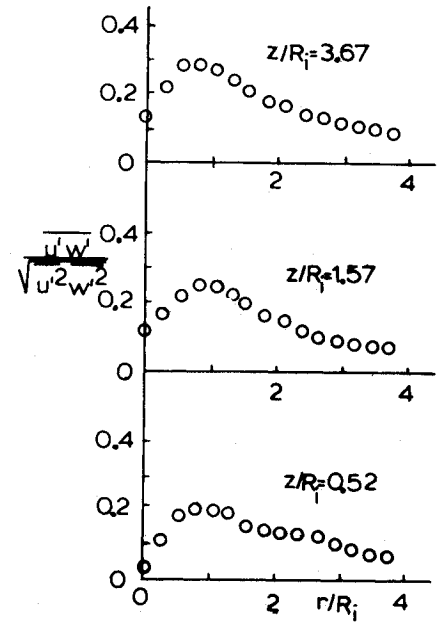

Fig. 12 Normalized axial-tangential velocity correlation profiles for coswirl.

Rhode[6] has shown that, under coswirl flow conditions, a recirculation zone does not exist. However, his calculation goes completely astray for downstream locations greater than 5 cm. Predictions by Sturgess et al.[20] have the same general character as those of Rhode[6] and Srinivasan and Mongia[18] but do not yield a recirculation zone (just). The differences between the results of Sturgess et al.[20] and Srinivasan and Mongia[18] are more due to the inlet boundary conditions than to grid differences. The boundary conditions employed in the numerical calculations reported here are shown in References 12-14.

In Fig. 10, we show the tangential velocity profiles at different axial locations. These profiles indicate that higher tangential velocities are measured by the LDV than by the hot wire at $z/R_i = 0.10$. These profiles are characterized by two velocity peaks located in the inner and outer jet regions. The LDV data indicate that the inner jet velocity peak is damped much more quickly than that measured with the hot wire. This can be observed in Fig. 10 at $z/R_i = 0.52$, 1.57, and 3.67. The outer jet velocity profile is preserved much longer than the inner jet one. The numerical results are in qualitative agreement with both the LDV and hot-wire data. The agreement with the LDV data is more satisfactory.

In Fig. 11, we show the turbulent intensity profiles at different axial locations along the combustor centerline. The LDV data only present a turbulent intensity peak, while the hot wire data show two peaks at $z/R_i = 0.52$. Downstream of this location, the two peaks merge into one, and the LDV and hot wire data are in good agreement although the turbulent intensities measured with the LDV are higher than those obtained with the hot wire. The numerical results are in qualitative agreement with the experimental data, but underpredict the turbulent intensity profiles in the inner jet region at $z/R_i = 1.57$ and 3.67.

In Fig. 12 we present the velocity correlations. These correlations are positive at the three axial locations shown in the figure and are not zero at the combustor center. The turbulence models employed in the calculations reported here assume that $\overline{u'w'} = 0$ at the centerline, since this correlation is assumed to be proportional to the corresponding mean flow strain rate which is zero at the centerline. Figure 12 also shows that the velocity correlations present a maximum at the interjet shear layer under coswirl flow conditions instead of the two peaks observed under counterswirl. Also, the magnitude

of the velocity cross-correlation is smaller for coswirl than for counterswirl. These results are consistent with the intensity of the interjet shear layer: as the magnitude of the outer swirl is decreased from counterswirl to coswirl flow conditions, the interjet shear layer intensity decreases.

As we mentioned previously, the LDV measurements reported herein are in reasonable good agreement with the hot-wire data of Vu and Gouldin[3] and the LDV results of Gouldin et al.[5] for counterswirl flow conditions. However, for coswirl flow conditions, our LDV data show a recirculation zone that has not been previously observed by either hot-wire or LDV measurements. A comparison of the LDV data reported here with those of Habib and Whitelaw[4] can only be qualitative because these investigators only studied weak swirl conditions, i.e., no recirculation zone at the combustor centerline was observed in their experiments. In addition, their combustor is provided with a sudden expansion. However, such a qualitative comparison reveals that, in the experiment of Habib and Whitelaw,[4] the turbulent intensity peaks at the interjet shear layer and is about 50%. The axial velocity profile was also observed to peak off the combustor centerline in the experiments presented here, as shown in Figs. 5 and 9. Thus, the general flow trends observed by Habib and Whitelaw[4] are qualitatively similar to those shown in this paper. A toroidal recirculation similar to the one reported here has also been observed by Yoon and Lilley[9] in a swirl combustor provided with a single swirling jet and a sudden expansion. The results were obtained with a five-hole pitot probe and indicate that the flowfield is very sensitive to the swirl vane angle and inlet boundary conditions.

The experimental data presented here, as well as those of other investigators, indicate that substantial errors can be introduced by perturbing the flow by means of a hot-wire probe[3] and that the flow is rather sensitive to the method employed to generate swirl. They also indicate that the swirl number is not the only parameter that characterizes swirling flows and that the inlet flow boundary conditions should be provided in future experiments so that they can be used to validate and improve turbulent models for swirling flows before they are employed to predict more complex geometrical arrangements possibly with chemical reactions.

Conclusions

A two-color laser Doppler velocimeter has been employed to measure the mean axial velocity, mean tangential velocity, turbulence intensity and velocity cross correlation profiles in a combustor under nonreacting, turbulent swirling flow conditions. Co- and counterswirl conditions have been measured and compared with experimental data obtained with hot wires. The measurements have also been compared with numerical results obtained by means of two two-equation turbulence models for the turbulence kinetic energy and the turbulent length scale. The comparison with the experimental data shows a satisfactory agreement among the hot-wire, LDV, and numerical data for the axial velocity profiles under counterswirl flow conditions. However, the tangential velocity of the inner jet and the turbulent intensity profiles show substantial differences. The numerical results indicate that turbulence generation occurs at the interjet shear layer and in the recirculation zone, while both sets of experimental data indicate that the turbulence kinetic energy peaks at the interjet shear layer. Under counterswirl flow conditions the velocity cross-correlations present two peaks: one is located at the interjet shear layer; the other is located near the combustor centerline. The locations of these peaks coincide with the locations of the steepest axial and tangential velocity gradients.

Under coswirl flow conditions the LDV data and numerical results show a one-celled toroidal recirculation zone that is not observed in the hot-wire data. The hot-wire data also show larger tangential velocity profiles than the LDV data and numerical results. They also show two turbulent intensity maxima that are not detected either numerically or in the LDV data. The velocity cross-correlation profiles are of less magnitude than the corresponding profiles under counterswirl flow conditions, and show similar trends to those of the turbulence intensity.

The numerical results are in qualitative agreement with the LDV measurements for both co- and counterswirl flow conditions. However, they use an isotropic eddy diffusivity and do not consider the effects of streamline curvature on the turbulence. The inclusion of these effects may yield more accurate results. Experimental information concerning the boundary conditions at the combustor inlet is needed, since small changes in these conditions cause large changes in the flowfield. More experimental results are also needed to verify the existence of a toroidal recirculation zone under coswirl flow conditions, and to assess whether the swirl number is the only parameter which defines the existence of a recirculation zone. It has been found numerically that different tangential velocity profiles may give the same swirl number, but different flow fields. The influence of the tangential velocity profile and modes of swirl generation should be addressed in the near future. Also, experiments should be carried out to measure the inlet flow boundary conditions so that validation checks of theoretical models for swirling flow can be undertaken.

Acknowledgments

The first author was supported by a Ford Motor Company Research Fund Grant. The second author's work was supported by the Office of Naval Research under contract No. N00014-80-C-0400. The authors would like to thank Prof. F. C. Gouldin of Cornell University for useful comments and suggestions concerning the vane design of the swirl generator.

References

[1] Syred, N. and Beer, J. M., "Combustion in Swirling Flows: A Review." *Combustion and Flame,* Vol. 23, 1974, pp. 143-201.

[2] Yetter, R. A. and Gouldin, F. C., "Exhaust Gas Emissions of a Vortex Breakdown Stabilized Combustor," paper presented at the Fall Meeting of the Western States Section of the Combustion Institute, Oct. 1976.

[3] Vu, B. T. and Gouldin, F. C., "Flow Measurements in a Model Swirl Flow," *AIAA Journal,* Vol. 20, 1982, pp. 652-659.

[4] Habib, M. A. and Whitelaw, J. H., "Velocity Characteristics of Confined Coaxial Jets with and without Swirl," *Journal of Fluids Engineering,* Vol. 102, 1980, pp. 47-53.

[5] Gouldin, F. C., Depsky, J. S., and Lee, S. L., "Velocity Field Characteristics of a Swirling Flow Combustor," AIAA Paper 83-0314, Jan. 1983.

[6] Rhode, D. L., "Predictions and Measurements of Isothermal Flowfields in Axisymmetric Combustor Geometries," Ph.D. Thesis, School of Mechanical and Aerospace Engineering, Oklahoma State University, Stillwater, Okla. 1981.

[7] Rhode, D. L., Lilley, D. G., and McLaughlin, D. K., "On the Prediction of Swirling Flowfields Found in Axisymmetric Combustor Geometries," *Journal of Fluids Engineering,* Vol. 104, 1982, pp. 378-384.

[8] Gupta, A. K., Beer, J. M., Louis, J. F., Busnaina, A. A., and Lilley, D. G., "Flow Aerodynamics Modeling of an MHD Swirl Combustor: Calculations and Experimental Verification," *Journal of Fluids Engineering,* Vol. 104, 1982, pp. 385-392.

[9] Yoon, H. K. and Lilley, D. G., "Five-Hole Pitot Probe Time-Mean Velocity Measurements in Confined Swirling Flows," AIAA Paper, 83-0315, Jan. 1983.

[10] Sommer, H. T., "Swirling Flow in a Research Combustor," AIAA Paper 83-0313, Jan. 1983.

[11] Kubo, I. and Goldin, F. C., "Numerical Calculations of Turbulent Swirling Flow, *Journal of Fluids Engineering,* Vol. 97, 1975, pp. 310-315.

[12]Ramos, J. I., "A Numerical Study of Incompressible, Turbulent, Confined, Swirling Flows. Part I: The Vortex Sheet Layer," Dept. of Mechanical Engineering, Carnegie-Mellon University, Pittsburgh, Pa., Rept. CO/80/4, 1980.

[13]Ramos, J. I., "A Numerical Study of Incompressible, Turbulent, Confined, Swirling Flows. Part II: The Effect of the Inner Piper Thickness," Dept. of Mechanical Enginering. Carnegie-Mellon University, Pittsburgh, Pa., Rept. CO/80/5, 1980.

[14]Ramos, J. I., "A Numerical Study of Turbulent Swirling Flows," Dept. of Mechanical Engineering, Carnegie-Mellon University, Pittsburgh, Pa., Rept. CO/81/2, 1981.

[15]Ramos, J. I., "A Numerical Study of Turbulent, Confined, Swirling Jets," *Numerical Methods in Laminar and Turbulent Flows*, Pineridge Press, Swansea, U.K., 1981, pp. 401-412.

[16]Ramos, J. I., "The Numerical Modelling of Swirling Flows in a Gas Turbine Combustor," *Refined Modelling of Flows*, Vol. 2, Presses de L'Ecole Nationale des Ponts et Chaussees, Paris, 1982, pp. 443-452.

[17]Ramos, J. I., "Turbulent Nonreacting Swirling Flows," *AIAA Journal*, Vol. 22, 1984, pp. 846-848.

[18]Srinivasan, R. and Mongia, H. C., "Numerical Computations of Swirling Recirculating Flow: Final Rept.," NASA CR-165186, 1980.

[19]Abujelala, M. T. and Lilley, D. G., "Confined Swirling Flow Predictions," AIAA Paper 83-0316, Jan. 1983.

[20]Sturges, G. J., Syed, S. A., and McManus, K. R., "Importance of Inlet Boundary Conditions for Numerical Simulation of Combustor Flows," AIAA Paper 83-1263, 1983.